VTT Technical Research Centre of Finland

Cell Splitting for Energy-Efficient Massive MIMO

Apilo, Olli; Lasanen, Mika; Wang, Jiaheng; Mämmelä, Aarne

Published in:
2017 IEEE 86th Vehicular Technology Conference (VTC-Fall)

DOI:
10.1109/VTCFall.2017.8288110

Published: 01/01/2018

Document Version
Peer reviewed version

Title	Cell Splitting for Energy-Efficient Massive MIMO
Author(s)	Apilo, Olli ; Lasanen, Mika ; Wang, Jiaheng ; Mämmelä, Aarne
Citation	Proceedings of 2017 IEEE 86th Vehicular Technology Conference (VTC-Fall) Institute of Electrical and Electronic Engineers IEEE IEEE 86th Vehicular Technology Conference, VTC-Fall 2017, Toronto, Canada, 24 – 27 September 2017
Date	21.5.2018
DOI	10.1109/VTCFall.2017.8288110
Rights	This article may be downloaded for personal use only.

Cell Splitting for Energy-Efficient Massive MIMO

Olli Apilo, Mika Lasanen, and Aarne Mämmelä
VTT Technical Research Centre of Finland Ltd
Kaitoväylä 1, P.O. Box 1100, FI-90571 Oulu, Finland
Email: {Olli.Apilo, Mika.Lasanen, Aarne.Mammela}@vtt.fi

Jiaheng Wang
National Mobile Communications Research Lab
Southeast University, Nanjing 210096, China
Email: jhwang@seu.edu.cn

***Abstract*—In this paper, we propose a novel cell splitting approach for massive multiple-input multiple-output (MIMO) base stations to improve energy efficiency. The user equipments (UEs) in the cell are divided into two groups based on their distances to the base station. These two UE groups are scheduled at different time slots, which effectively splits a cell into inner and outer cells. The number of transmitting and receiving antennas together with the downlink and uplink transmission powers are adapted according to the number of cell edge and center UEs to maximize energy efficiency. We propose two algorithms to optimize the number of antennas and transmission powers. Cell splitting is able to reach energy efficiency (EE) gain of 11-41 % depending on the UE density when compared to a conventional load-adaptive massive MIMO system. The inevitable loss of cell edge UE rates can be controlled by setting a target UE rate, which also reduces the search space of the optimization algorithm.**

I. Introduction

5G mobile networks should improve the performance of existing IMT-Advanced networks in terms of area traffic capacity, data rate, spectrum and energy efficiency, connection density, latency, and mobility [1]. Massive multiple-input multiple-output (MIMO) [2] is a strong candidate to fulfill the 5G area traffic capacity and spectral efficiency targets [3]. In massive MIMO M antennas are used to serve K single-antenna user equipments (UEs). When $M >> K$, it is possible to form narrow beams towards the UEs. This provides two obvious benefits: 1) the inter-user interference becomes very small allowing many UEs to be served with the same time-frequency resource, 2) per-antenna transmission power becomes very low enabling the use of low-cost, low-power radio frequency (RF) components [4]. The main restriction of the massive MIMO performance is pilot contamination that is caused by the re-use of the same pilot symbols in adjacent cells [2].

Although massive MIMO can operate efficiently with low transmitted power, the RF and baseband processing power consumption is significant due to the large number of antenna elements. Energy efficiency of massive MIMO has recently been analyzed in [5]–[7]. According to these studies, the energy efficiency (EE) (in bits/J) as a function of M is concave. Thus for a given number of served UEs, there is an EE-maximizing number of antennas. It was shown in [8], [9] that adapting the number of active antennas to the number of served UEs can provide significant EE gain when the number of UEs varies according to a realistic traffic profile. On the other hand, the EE function is also concave with respect to the number of served UEs [6]. If the number of UEs in the cell exceeds the EE-optimal number of UEs, K_{EE}, the maximal level of energy efficiency can be maintained by round-robin scheduling of the UEs. However with this approach, the cell sum rate stays constant when $K > K_{\mathrm{EE}}$ which may not be acceptable from the area traffic capacity point of view.

Motivated by the need for efficient massive MIMO solutions under high traffic load, we propose that the UEs are divided into two groups that are scheduled at different time slots. The grouping criteria is the distance to the serving base station (BS) which splits the cell into inner and outer cells. Cell splitting reduces the power consumption because less active antennas are needed to serve less UEs. When the equal rate power control is used, the average signal-to-interference-plus-noise ratio (SINR) and correspondingly data rates for cell center and cell edge UEs are increased and decreased, respectively. The cell edge data rate loss can be controlled by setting a target rate that should be reached by all UEs. We provide an algorithm that selects the cell edge radius, the number of active antennas, and the transmission power for different number of UEs. We show that the significant EE gain can be reached also with a fixed cell edge radius with considerably reduced complexity. Proposed cell splitting can be seen as a special case of fractional time reuse [10] with only two reuse sets. However, unlike in [10] our proposal is actually trading off cell edge spectral efficiency for energy efficiency. As far as we know, fractional time reuse has not earlier been proposed for improving energy efficiency.

The rest of the paper is organized as follows: The multi-cell system model is described in Section II. The idea of the cell splitting is described in Section III, which also includes the brute force algorithm and approximate simplifications to maximize the average energy efficiency in a massive MIMO system with cell splitting. The numerical results are given in Section IV. Finally, conclusions are drawn in Section V.

II. System Model

We consider a time domain duplex hexagonal multi-cell massive MIMO system with J cells having inter-BS distance a. To alleviate the pilot contamination problem, cells are divided into sets using the same pilot symbols. The number of different pilot reuse sets is given by the pilot reuse factor τ. Each BS adapts its number of active antennas $m \leq M$ according to the number of scheduled UEs. The UEs are uniformly distributed in the cell and their number is Poisson distributed according to $K \sim \mathrm{Pois}(\lambda_h)$ where the average

number of UEs is $\lambda_h = c(h)\hat{K}$. The average number of UEs during the busy hour $\hat{K}$ is multiplied by the hourly traffic level multiplier $c(h) \leq 1$ that is defined according to [11].

The channel is assumed reciprocal and static during a time-frequency block of U symbols (resource elements). The channel between UE k and its serving BS is given by $m \times 1$ vector of channel coefficients $\mathbf{h}^{(k)}$ whose each element is complex Gaussian distributed as $h_n^{(k)} \sim \mathcal{CN}(0, \Lambda(d)), \forall n = 1, \ldots, m$ where $\Lambda(d) = \kappa/d^\alpha, d \geq d_{\min}$ is the path loss. The propagation scenario is characterized by the constant κ, the path loss exponent α, and the minimum distance to the BS $d_{\min}$. The first $\tau K < U$ symbols are reserved for uplink (UL) pilots and the remaining $U - \tau K$ symbols are divided evenly for UL and downlink (DL) data. No DL pilots are needed due to the channel reciprocity [12]. The fraction of time reserved for pilots, UL and DL are denoted by $\zeta_p = (\tau K)/U$, $\zeta_u = (U - \tau K)/(2U)$ and $\zeta_d = (U - \tau K)/(2U)$, respectively.

Within each time slot, the data rates for each UE are set to be equal using a per-UE power control described in [6]. Also the average received signal-to-noise ratio (SNR) ρ is set to be equal in DL and UL such that

$$\rho = \frac{mP_{\text{Tx}}}{B\sigma^2 E\left[(\Lambda(d))^{-1}\right] K} = \frac{P_{\text{Tx, UE}}}{B\sigma^2 E\left[(\Lambda(d))^{-1}\right]} \tag{1}$$

where σ^2 is the additive white Gaussian noise (AWGN) spectral density and $E\left[(\Lambda(d))^{-1}\right]$ is the average inverse channel attenuation. In practical systems, the DL and UL transmission powers mP_{Tx} and $P_{\text{Tx, UE}}$ are restricted giving an upper bound to ρ. For example, ρ is bounded by the maximum UL transmission power when $K < mP_{\text{Tx}}/P_{\text{Tx, UE}}$ which is the case in macro cells for practical number of served UEs. The resulting average per-UE rate R is given by

$$R = R_{\text{dl}} + R_{\text{ul}} = \frac{U - \tau K}{U} B \log_2(1 + \gamma) \tag{2}$$

where B is the channel bandwidth and γ is the received SINR. When the effects of pilot contamination and imperfect channel estimation are taken into account, the SINR with zero-forcing (ZF) processing can be given as [6]

$$\gamma = \frac{1}{\mathcal{I}_{\text{PC}} - 1 + \left(\mathcal{I}_{\text{PC}} + \frac{1}{\rho K \tau}\right)\frac{1 + K\rho\mathcal{I}}{\rho(m-K)} - \frac{K\mathcal{I}_{\text{PC}^2}}{m-K}}. \tag{3}$$

$\mathcal{I}$, $\mathcal{I}_{\text{PC}}$, and $\mathcal{I}_{\text{PC}^2}$ are the relative interferences defined using the mean ratio of path losses between the interfering cell l and serving cell j, $\mathcal{I}_{jl} = E[\Lambda(d_l)/\Lambda(d_j)]$ where d_l and d_j are the distances to interfering and serving BSs, respectively. The sum of relative interference from all cells $\mathcal{I}$ is defined as $\mathcal{I} = \sum_{l=1}^{J} \mathcal{I}_{jl}$. The interference terms $\mathcal{I}_{\text{PC}}$ and $\mathcal{I}_{\text{PC}^2}$ are given as $\mathcal{I}_{\text{PC}} = \sum_{l \in \mathcal{Q}_j} \mathcal{I}_{jl}$ and $\mathcal{I}_{\text{PC}^2} = \sum_{l \in \mathcal{Q}_j} \mathcal{I}_{jl}^2$ where $\mathcal{Q}_j \subset \{1, \ldots, J\}$ is the set of cells sharing the same pilot symbols.

The power consumption model used in this paper follows the one presented in [9] which combines earlier power consumption models for power amplifiers [13], other BS components [6], [14], and UEs [15]. The total system power consumption is defined as

$$P = \frac{P_{\text{PA}} + P_{\text{RF}} + P_{\text{BB}} + P_{\text{OH}}}{\eta_{\text{PS}}} + KP_{\text{UE}} \tag{4}$$

where P_{PA} is the average power amplifier (PA) power consumption, P_{RF} is the RF circuit power consumption, P_{BB} is the baseband power consumption, P_{OH} is the overhead power consumption of platform control and network processing, η_{PS} is the power conversion efficiency of the power system, and P_{UE} is the average consumed power of each UE.

The average consumed PA power is given by

$$P_{\text{PA}} = \frac{2\zeta_d m P_{\text{Tx}} \sqrt{\xi} \text{erf}\left(\sqrt{\xi}\right)}{\sqrt{\pi}\left(1 - e^{-\xi}\right)} \tag{5}$$

where $\xi = P_{\text{Tx}}^{\max}/P_{\text{Tx}}$ is the output power back-off. The RF circuit power consumption is modelled as

$$P_{\text{RF}} = m\left(P_{\text{FRQ}} + \zeta_d P_{\text{RF,DL}} + \zeta_u P_{\text{RF,UL}}\right) + \sqrt{m} P_{\text{CLK}} \tag{6}$$

where P_{FRQ} is the power required for frequency synthesis, $P_{\text{RF,DL}}$ and $P_{\text{RF,UL}}$ are the power consumption of RF transmission and reception circuits, and P_{CLK} is the power required for clock generation.

The digital baseband power consumption can be given as

$$\begin{aligned} P_{\text{BB}} =& m\left(P_{\text{OFDM}} + \zeta_p P_{\text{SYNC}}\right) + \frac{KR}{\epsilon_{\text{FEC}}} + KP_{\text{MOD}}\left(\frac{R}{\hat{R}}\right)^{1.5} \\ &+ \frac{BK\left(K^2/3 + 3mK + m(1 + 2U)\right)}{\epsilon_{\text{DSP}} U} \end{aligned} \tag{7}$$

where P_{OFDM} is the power consumption of multicarrier processing, P_{SYNC} is the power consumption of synchronization, ϵ_{FEC} is the channel coding energy efficiency (in bit/J), $\hat{R}$ is the reference data rate, P_{MOD} is the power consumption of modulation, and ϵ_{DSP} is the energy efficiency of digital signal processing (DSP) (in floating point operations (flop) per joule). Power consumption of overhead processing is given as

$$P_{\text{OH}} = \sqrt{m} K^{0.2}\left(\zeta_d P_{\text{CDL}} + \zeta_u P_{\text{CUL}}\right) + R/\epsilon_{\text{NET}} \tag{8}$$

where P_{CDL} and P_{CUL} are the platform control processing powers for DL and UL, respectively. The energy efficiency for network processing is ϵ_{NET}.

Finally, the UE power consumption is modelled as

$$\begin{aligned} P_{\text{UE}} =& \zeta_d\left(P_{\text{DL}} + P_{\text{Rx,RF}}\left(P_{\text{Rx}}\right)\right) + P_{\text{Rx,BB}}\left(R/2\right) \\ &+ \zeta_u\left(P_{\text{UL}} + P_{\text{Tx,RF}}\left(P_{\text{Tx,UE}}\right)\right) + P_{\text{ON}} \end{aligned} \tag{9}$$

where P_{DL} is the constant power consumed when receiving data, $P_{\text{Rx}} = \rho B \sigma^2$ is the average received power, P_{UL} is the constant power consumed when transmitting data, and P_{ON} is the constant power consumed when the cellular subsystem is turned on. The variable terms in (9), i.e. power consumptions of DL RF processing $P_{\text{Rx,RF}}\left(P_{\text{Rx}}\right)$, DL baseband processing $P_{\text{Rx,BB}}\left(R_{\text{dl}}\right)$, and UL RF processing $P_{\text{Tx,RF}}\left(P_{\text{Tx,UE}}\right)$, are defined in Table 4 of [15].

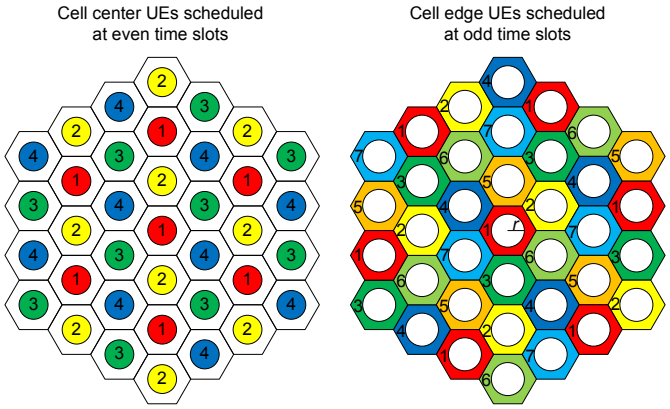

Fig. 1. Pilot reuse pattern when $\tau_c = 4$ and $\tau_e = 7$.

III. Massive MIMO cell splitting

Earlier works have shown that the energy efficiency is concave with respect to the number of served UEs [6], [9]. The EE-optimal number of UEs K_{EE} depends on the system assumptions and especially on the used power consumption model. When $K > K_{\text{EE}}$, a straightforward way to preserve the maximum energy efficiency is to restrict the number of served UEs to K_{EE} and use round-robin scheduling. However from mobile operator point of view, this is rarely a satisfactory approach because the cell sum rate stays fixed even with the increasing number of UEs in the cell.

As an improvement to simple round-robin scheduling, we propose that UEs are divided into cell center and edge UEs which are served in successive time slots. UE k is considered as a cell edge UE and served during outer cell time slots if its distance to the serving BS fulfills $d_k > r$ where r is the cell edge radius. Similarly, UE i is considered as a cell center UE if $d_i \leq r$. The number of active antennas m and the average received SNR ρ are adapted for each time slot. This makes it possible to optimize the system separately for the inner and outer cells. Some additional EE gain can be achieved by adapting the cell edge radius to the total number of UEs in the cell. When all cells in the system are synchronized and use the same time slots for center and edge UEs, it is possible to have different pilot reuse factors in inner and outer cells. This is illustrated in Fig. 1 where pilot reuse factor $\tau_c = 4$ in the inner cells and pilot reuse factor $\tau_e = 7$ in the outer cells. The different numbers and colors in Fig. 1 correspond to different sets of orthogonal pilots. For the rest of this paper we use subscript $_e$ and superscript $^{(e)}$ to refer variables valid during cell edge time slots. Similarly, subscript $_c$ and superscript $^{(c)}$ refer to cell center time slots.

Our proposed cell splitting reduces the number of active antennas and the number of scheduled UEs per time slot. This reduces consumed power significantly because the power consumption model presented in Section II has strong dependence on m and K. The drawback of our proposed method is that the cell sum rate and especially the cell edge UE rate is reduced. However, the cell edge UE rate reduction can be controlled by setting the minimum allowed rate R_t accordingly.

The maximization of the average energy efficiency can be formulated as

$$\begin{aligned} &\max_{\substack{m_e, m_c \leq M, \\ \rho_e, \rho_c \leq \rho_{\max}, \\ d_{\min} \leq r < r_{\max}}} \hat{\epsilon} = \sum_{k=0}^{\infty} \epsilon_k p_K(k) \\ &= \sum_{k=0}^{\infty} \sum_{k_e=0}^{k} \frac{k_e R_e + (k-k_e) R_c}{P_e + P_c} p_{K_e}(k_e | K=k) p_K(k) \\ &\text{subject to} \quad R_e \geq R_t \end{aligned} \tag{10}$$

where $p_K(k) = \lambda_h^k e^{-\lambda}/k!$ and

$$p_{K_e}(k_e | K=k) = \binom{k}{k_e} \left(1 - \frac{A_c}{A}\right)^k \left(\frac{A_c}{A}\right)^{k-k_e}. \tag{11}$$

The cell area is given by $A = 2\sqrt{3}(a/2)^2 - \pi d_{\min}^2$ and the cell center area is given by $A_c = \pi r^2 - \pi d_{\min}^2$. The cell edge rate R_e and power P_e can be derived from Eqs. (2) and (4) by applying the parameters $\{\rho_e, m_e, \tau_e, K_e\}$ and restricting $d > r$. The cell center rate R_c and power P_c can be derived in the same way by applying the parameters $\{\rho_c, m_c, \tau_c, K_c\}$ and restricting $d \leq r$. When $R_t = 0$, the UE rate is unrestricted and the energy efficiency is maximized. The cell edge UE rate can be increased by using more antennas, transmitting with a higher power, or by decreasing the cell edge radius, which increases the average SINR.

As mentioned in Section II, the upper limit for the per-antenna received SNR $\rho_{\max}$ is bounded by the maximum UL transmission power $P_{\text{Tx,UE}_{\max}}$ for practical number of served UEs in macro cells. For a given r and $P_{\text{Tx,UE}_{\max}}$, we can get $\rho_{\max}$ from (1). On the other hand, the UE rate constraint sets a lower limit to ρ that can be solved from (2) by setting $R_e = R_t$. The resulting minimum per-antenna received SNR is

$$\rho_{\min} = \frac{-\gamma_t K_e \left(\tau_e I_{\text{PC}}^{(e)} + I_e\right) \pm \sqrt{\left(\gamma_t K_e (\tau_e I_{\text{PC}}^{(e)} + I_e)\right)^2 - 4 a_t \gamma_t}}{2 a_t} \tag{12}$$

where $\gamma_t = 2^{R_t U/(B(U-\tau_E K_e))} - 1$ and

$$\begin{aligned} a_t = \gamma_t \big(&K_e \tau_e (m_e - K_e) I_{\text{PC}}^{(e)} - K_e \tau_e (m_e - K_e) + \\ &K_e^2 \tau_e I_e I_{\text{PC}}^{(e)} - K_e^2 \tau_e I_{\text{PC}^2}^{(e)} \big) - K_e \tau_e (m_e - K_e). \end{aligned} \tag{13}$$

When there are no positive roots from (12) or $\rho_{\min} > \rho_{\max}$, the target UE rate cannot be reached and the number of antennas has to be increased. By setting $\rho_{\max}$ into (2) and solving m_e from $R_e = R_t$, it is possible to derive the minimum number of antennas $m_{\min}$ that still can reach the target UE rate as

$$m_{\min} = \left\lceil \frac{\gamma_t K_e I_{\text{PC}^2}^{(e)} \rho_{\max} - \frac{\left(\gamma_t I_{\text{PC}}^{(e)} \rho_{\max} K_e \tau_e + \gamma_t\right)(1 + K_e \rho_{\max} I_e)}{\rho_{\max} K_e \tau_e}}{\gamma_t I_{\text{PC}}^{(e)} \rho_{\max} - \gamma_t \rho_{\max} - \rho_{\max}} + K_e \right\rceil. \tag{14}$$

If $m_{\min} > M$, the target rate cannot be reached with the available antennas. In this case, the only way is to reduce the cell edge radius. The maximum cell edge radius $r_{\max}$ that still fulfills the target UE rate can be solved numerically for the given K_e from $R_e = R_t$ with $P_{\text{Tx,UE}} = P_{\text{Tx,UE}_{\max}}$ and $m_e = M$. If $P_{\text{Tx,UE}_{\max}}$ or M are low enough, it is possible that $r_{\max} < d_{\min}$. In this case, the proposed cell splitting approach cannot guarantee the target UE rate when the number of cell edge UEs is larger than $K_e - 1$. In this case, conventional scheduling can be used by setting $r = d_{\min}$ and scheduling all UEs in each time slot.

As seen from (2), the optimization variables m and ρ are both in the numerator and denominator making it intractable to find a closed-form solution for (10). If we quantize r with a step size $0 < b \leq d_{\min}$ such that the number of possible cell edge radius values is $Q = \lfloor (r_{\max} - d_{\min})/b \rfloor$, the optimization problem can be solved numerically by exhaustive search. For a given K, the algorithm for searching the EE-optimal cell edge radius $\hat{r}$ and $K \times Q$ matrices $\hat{\mathbf{m}}^{(e)}$, $\hat{\mathbf{m}}^{(c)}$, $\hat{\rho}^{(e)}$, and $\hat{\rho}^{(c)}$ is given as follows

Solve $r_{\max}$ from $R_e = R_t$ with $P_{\text{Tx,UE}} = P_{\text{Tx,UE}_{\max}}$ and $m_e = M$
$Q \leftarrow \max\left(\lfloor (r_{\max} - d_{\min})/b \rfloor, 1\right)$, $\epsilon_K \leftarrow 0$
for $q = 1$ to Q **do**
  $r \leftarrow d_{\min} + (q-1)b$, $\epsilon_r \leftarrow 0$
  for $k_e = 0$ to K **do**
    Calculate $m_{\min}$ using (14)
    $m_e \leftarrow \min(m_{\min}, M)$, $\epsilon_e \leftarrow 0$, $\epsilon_{\max} = 0$
    while ($\epsilon_e \leq \epsilon_{\max}$ **and** $m_e \leq M$) **do**
      Calculate $\rho_{\min}$ using (12)
      Solve $\max_{\rho_{\min} < \rho_e \leq \rho_{\max}} (k_e R_e)/P_e$
      $\epsilon_e \leftarrow (k_e R_e)/P_e$
      if $\epsilon_e > \epsilon_{\max}$ **then**
        $\hat{m}^{(e)}_{k_e,q} \leftarrow m_e$, $\hat{\rho}^{(e)}_{k_e,q} \leftarrow \rho_e$, $\epsilon_{\max} \leftarrow \epsilon_e$
      end if
      $m_e = m_e + 1$
    end while
    $\epsilon_c \leftarrow 0$, $\epsilon_{\max} = 0$, $m_c = k_e + 1$
    while $\epsilon_c \leq \epsilon_{\max}$ **do**
      Solve $\max_{\rho_c \leq \rho_{\max}} ((K - k_e)R_c)/P_c$
      $\epsilon_c \leftarrow ((K - k_c)R_c)/P_c$
      if $\epsilon_c > \epsilon_{\max}$ **then**
        $\hat{m}^{(c)}_{K-k_e,q} \leftarrow m_c$, $\hat{\rho}^{(c)}_{K-k_e,q} \leftarrow \rho_c$, $\epsilon_{\max} \leftarrow \epsilon_c$
      end if
      $m_c = m_c + 1$
    end while
    $m_e \leftarrow \hat{m}^{(e)}_{k_e,q}$, $m_c \leftarrow \hat{m}^{(c)}_{K-k_e,q}$
    $\rho_e \leftarrow \hat{\rho}^{(e)}_{k_e,q}$, $\rho_c \leftarrow \hat{\rho}^{(c)}_{K-k_e,q}$
    $\epsilon_r = \epsilon_r + \frac{k_e R_e + (k-k_e)R_c}{P_e + P_c} \cdot p_{K_e}(k_e | K = k)$
  end for
  if $\epsilon_r > \epsilon_k$ **then**
    $\epsilon_k = \epsilon_r$, $\hat{r} = r$
  end if
end for.

The constraint on the cell edge UE rate actually reduces the search space of the brute force algorithm as the upper limit for r is decreased and the lower limits for m_e and ρ_e are increased. However when the propagation environment changes, there may be a need to run the optimization algorithm also during run-time. For these cases, some approximate simplifications can be done:

A) Use the alternating optimization algorithm for finding $\{\hat{m}^{(e)}_{k_e,q}, \hat{\rho}^{(e)}_{k_e,q}\}$ and $\{\hat{m}^{(c)}_{k_e,q}, \hat{\rho}^{(c)}_{k_e,q}\}$.
B) Use fixed r for all $K = 1, \ldots, K_{\max}$.

When simplification A) is used, m_e and ρ_e are solved sequentially until a local optimum is reached:

1) Calculate $m_{\min}$ using (14).
2) Set $m_e \leftarrow m$ where $m_{\min} \leq m < M$.
3) Calculate $\rho_{\min}$ using (12).
4) Solve $\max_{\rho_{\min} < \rho_e \leq \rho_{\max}} (k_e R_e)/P_e$.
5) Using ρ_e, solve $\max_{m_{\min} < m_e \leq M} (k_e R_e)/P_e$.
6) If m_e has changed from the previous iteration, go to Step 3.

The above algorithm has converged to a local optimum when m_e is unchanged from the previous iteration. m_c and ρ_c can be solved similarly with lower limits set to $\rho_{\min} = 0$ and $m_{\min} = K_c + 1$. If further complexity reduction is needed, it is also possible to fix the cell edge radius as in simplification B). In this case the optimal m_e, m_c, ρ_e, and ρ_c have to solved only once for each K. Obviously, alternating optimization algorithm can be applied also to simplification B).

IV. Numerical results

The numerical parameter values shown in Table I are used in simulations. The parameter values are mostly reused from [9]. The values for pilot reuse factor are selected based on extensive simulations such that they provide the high energy efficiency over a wide range of $\hat{K}$ values. In the reference cases with no cell splitting, we set $r = d_{\min}$, all UEs are considered as cell edge UEs and the pilot reuse factor is 7.

The average energy efficiency as a function of average number of UEs during the busy hour $\hat{K}$ is shown in Fig. 2. Cell splitting without the UE rate constraint is able to reach EE gain of 11-41 % depending on the UE density. As can be seen from Figs. 3 and 4, the EE gain is achieved by significant power consumption reduction and at the same time the cell sum rate is only moderately degraded. The power consumption reduction is caused by decreasing m and K per time slot, both of which have a nonlinear dependency on the power consumption.

The average rate per UE is shown in Fig. 5. Without any rate targets, the cell edge UE rate decreases to 44-49 % of the UE rate without cell splitting. The cell edge UE rate can be increased by setting a rate target. However, this increases the power consumption, as seen from Fig. 3, mostly because more active antennas are needed to fulfill the rate target at the cell edge. This in turn reduces the energy efficiencies that is illustrated in Fig. 2. Because of the used equal rate power control, the instantaneous rates at the cell center are approximately doubled which compensates the halving of

TABLE I
PARAMETER VALUES FOR SIMULATIONS.

Parameter	Value
Distance between BSs, a	500 m
Minimum distance between a UE and a BS, $r_{\min}$	35 m
Pilot reuse factor, $\{\tau_c, \tau_e\}$	$\{4, 7\}$
Number of symbols in time slot, U	1800
Path loss constant, κ	$10^{-3.53}$
Path loss exponent, α	3.76
Number of cells in the system,[1] J	37
Transmission bandwidth, B	20 MHz
Noise spectral density, σ^2	-169 dBm/Hz
Power conversion efficiency, η_{PS}	0.846
Maximum UE transmission power, $P_{\text{Tx,UE}_{\max}}$	0.2 W
Maximum PA output power, $P_{\text{Tx}}^{\max}$	1.59 W [2]
Frequency synthesis power, P_{FRQ}	102 mW
RF transmission power, $P_{\text{RF,DL}}$	287 mW
RF reception power, $P_{\text{RF,UL}}$	413 mW
Clock generation power, P_{CLK}	61 mW
Multicarrier processing power, P_{OFDM}	237 mW
Synchronization power, P_{SYNC}	52 mW
Channel coding energy efficiency, ϵ_{FEC}	630 Mbit/J
Reference data rate, $\hat{R}$	75.4 Mbit/s
Modulation power, P_{MOD}	36.4 mW
DSP energy efficiency, ϵ_{DSP}	15.5 Gflop/J
DL platform control power, P_{CDL}	104 mW
UL platform control power, P_{CUL}	38.6 mW
DL network processing energy efficiency, ϵ_{NET}	271 Mbit/J
Maximum number of UEs in the cell, $K_{\max}$	139

[1] The center cell in Fig. 1, which represents any cell in the symmetric multi-cell scenario, is considered.
[2] Corresponds to the case when $m = 2$, $K = 1$, and PA back-off is 12 dB.

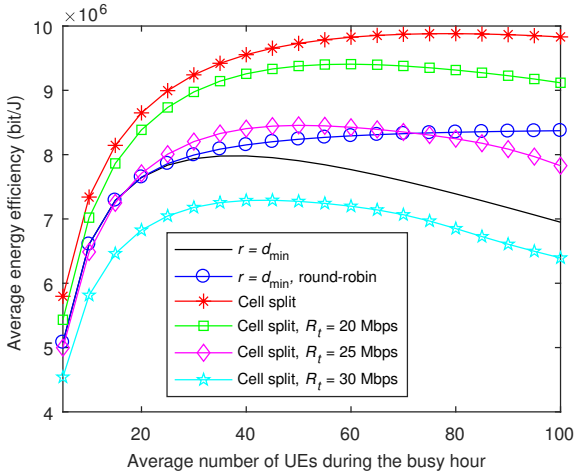

Fig. 2. Average energy efficiency as a function of $\hat{K}$.

available time slots for the cell center UEs. Thus, cell splitting does not cause rate reduction for cell center UEs. The target rate controls the trade-off between the EE gain and cell edge UE rate reduction. For example with $R_t = 25$ Mbps, the EE

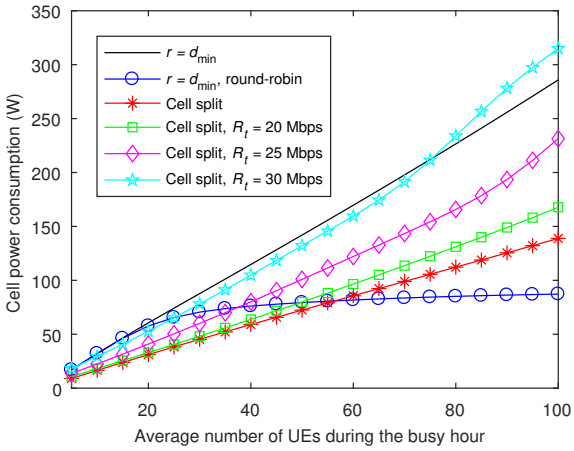

Fig. 3. Power consumption as a function of $\hat{K}$.

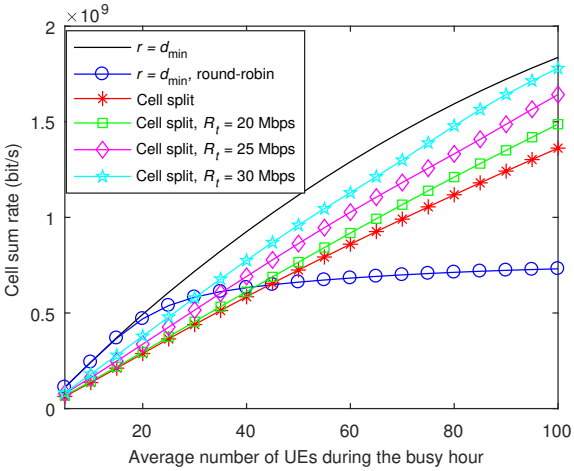

Fig. 4. Cell sum rate as a function of $\hat{K}$.

gain for high UE density ($\hat{K} = 70$) is 10 % with the cell edge UE rate reduction of 32 %. It should be noted that equal rate power control provides very good cell edge data rates even with cell splitting when compared to legacy 4G systems.

The simplifications presented in Section III are able to reduce the complexity of the optimization problem considerably. This is illustrated in Table II where the relative execution times of different simplifications are presented with respect to the complexity of the brute force algorithm. Even though the complexity reduction is significant when fixed r is used, the EE performance is only slightly degraded. This is shown in Fig. 6 where average energy efficiency vs. $\hat{K}$ is depicted for different simplifications. For Fig. 6, we have selected r such that 50 % and 35 % of the UEs are in the cell center when $R_t = 0$ and $R_t = 25$ Mbps, respectively. In general, r should be decreased when R_t is increased because it makes the average SINR more favorable for cell edge UEs.

V. CONCLUSIONS

We have proposed a simple cell splitting approach for massive MIMO base stations to improve energy efficiency.

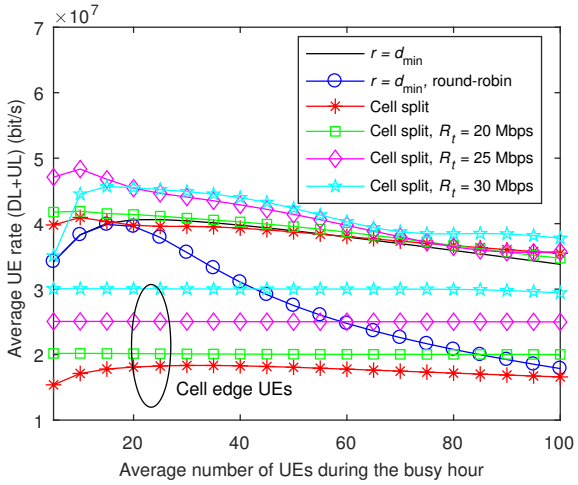

Fig. 5. UE rate as a function of $\hat{K}$.

TABLE II
RELATIVE EXECUTION TIMES OF DIFFERENT SIMPLIFICATIONS.

	Brute force	Altern. opt.	Fixed r	Fixed r + Altern. opt.
$R_t = 0$	100 %	7.4 %	0.58 %	0.053 %
$R_t = 20$ Mbps	27 %	6.6 %	0.28 %	0.044 %
$R_t = 25$ Mbps	17 %	5.2 %	0.24 %	0.044 %

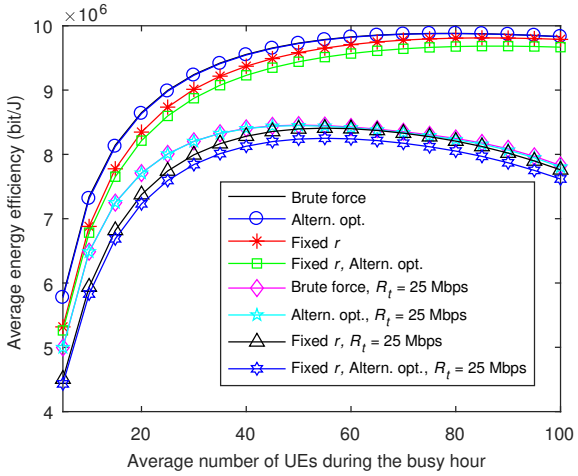

Fig. 6. Average energy efficiency as a function of $\hat{K}$ for different simplifications.

Cell splitting is implemented by dividing the UEs into two groups based on their distance to the base station. These two UE groups are scheduled at different time slots, which reduces the number of active antennas and served UEs per time slot. This results in significant reduction in power consumption when compared to the case where all UEs in the cell are served at the same time slot. We present an algorithm to solve the EE optimum number of antennas and the transmission powers for a given number of UEs in the inner and outer cell. The algorithm solves also the optimal cell edge radius for a given total number of UEs in the cell. These optimum parameter values can be calculated in the cell design phase if there is prior knowledge of the propagation environment. The execution time of the algorithm can be reduced to a small fraction if the cell edge radius is kept fixed. This results in slight performance degradation but enables the parameter solving during network operation.

Cell splitting without rate constraints is able to reach EE gain of 11-41 % depending on the UE density when compared to the conventional massive MIMO with load-adaptive number of antennas and transmission power. The EE gain comes with the price of reduced cell edge data rate that is caused by halving of the available time resources and degradation of the average SINR. The EE gain can be traded off for improved cell edge performance by setting a target UE rate.

ACKNOWLEDGMENT

The work was done in the TT5G project that is partly funded by Academy of Finland (decision number 284728).

REFERENCES

[1] *IMT vision: Framework and overall objectives of the future development of IMT for 2020 and beyond*, ITU-R Recommendation M.2083-0, Sep. 2015.
[2] T. L. Marzetta, "Noncooperative cellular wireless with unlimited numbers of base station antennas," *IEEE Trans. Wireless Commun.*, vol. 9, no. 11, pp. 3590–3600, Nov. 2010.
[3] F. Boccardi, R. W. Heath Jr., A. Lozano, T. L. Marzetta, and P. Popovski, "Five disruptive technology directions for 5G," *IEEE Commun. Mag.*, vol. 52, no. 2, pp. 74–80, Feb. 2014.
[4] E. G. Larsson, O. Edfors, F. Tufvesson, and T. L. Marzetta, "Massive MIMO for next generation wireless systems," *IEEE Commun. Mag.*, vol. 31, no. 2, pp. 160–171, Feb. 2014.
[5] L. Zhao, K. Li, K. Zheng, and M. O. Ahmad, "An analysis of the tradeoff between the energy and spectrum efficiencies in an uplink massive MIMO-OFDM system," *IEEE Trans. Circuits Syst. II*, vol. 62, no. 3, pp. 291–295, Mar. 2015.
[6] E. Björnson, L. Sanguinetti, J. Hoydis, and M. Debbah, "Optimal design of energy-efficient multi-user MIMO systems: Is massive MIMO the answer?" *IEEE Trans. Wireless Commun.*, vol. 14, no. 6, pp. 3059–3075, Jun. 2015.
[7] Y. Xin, D. Wang, J. Li, H. Zhu, J. Wang, and X. You, "Area spectral efficiency and area energy efficiency of massive MIMO cellular systems," *IEEE Trans. Veh. Technol.*, vol. 65, no. 5, pp. 3243–3254, May 2016.
[8] M. M. A. Hossain, C. Cavdar, E. Björnson, and R. Jäntti, "Energy-efficient load-adaptive massive MIMO," in *Proc. IEEE Globecom*, 2015.
[9] O. Apilo, M. Lasanen, and A. Mämmelä, "Unequal power amplifier dimensioning for adaptive massive MIMO base stations," in *Proc. IEEE VTC Spring*, 2016.
[10] C. He *et al.*, "Co-channel interference mitigation in MIMO-OFDM system," in *Proc. WiCom*, 2007, pp. 204–208.
[11] *Energy efficiency analysis of the reference systems, areas of improvements and target breakdown*, EARTH Deliverable D2.3 V2.0, 2012.
[12] E. Björnson, E. G. Larsson, and M. Debbah, "Massive MIMO for maximal spectral efficiency: How many users and pilots should be allocated?" *IEEE Trans. Wireless Commun.*, vol. 15, no. 2, pp. 1293–1308, Feb. 2016.
[13] H. Ochiai, "An analysis of band-limited communication systems from amplifier efficiency and distortion perspective," *IEEE Trans. Commun.*, vol. 61, no. 4, pp. 1460–1472, Apr. 2013.
[14] C. Desset, B. Debaillie, and F. Louagie, "Modeling the hardware power consumption of large scale antenna systems," in *Proc. IEEE OnlineGreenComm*, 2014.
[15] M. Lauridsen, L. Noël, T. B. Sørensen, and P. Mogensen, "An empirical LTE smartphone power model with a view to energy efficiency evolution," *Intel Technol. Journal*, vol. 18, no. 1, pp. 172–193, Jan. 2014.